PHENOMENOLOGICAL STUDY OF THE LIQUID PHASE PENETRATION ON DIESEL SPRAYS

Simón Martínez-Martínez

Universidad Autónoma de Nuevo León
Facultad de Ingeniería Mecánica y Eléctrica
Pedro de Alba s/n, 66450 San Nicolás de los Garza, N. L., México
tel.:+52 81 14920362, fax: +52(81)83320904
e-mail: simartin@gama.fime.uanl.mx

José Manuel Riesco-Ávila and Armando Gallegos-Muñoz

Universidad de Guanajuato
Facultad de Ingeniería Mecánica, Eléctrica y Electrónica
Tampico 912,36730 Salamanca Guanajuanto, México
tel.: +52 464 6480911, fax: +52 464 6472400
e-mail: riesco@salamanca.ugto.mx

Abstract

The phenomenological characterization of the liquid phase penetration on the diesel spray through the combustion chamber is very important to prevent and to reduce the pollution emission on the heavy duty Diesel engines as well as new combustion chambers design, for this reason, this work has concentrated on the characterization of the macroscopic behavior of the liquid phase penetration of diesel spray. The main purpose of this research is to define the influence of the nozzle hole diameter, injection pressure, gas density and temperature in diesel spray penetration on evaporating conditions. The results show that the nozzle hole diameter and thermodynamics properties as the gas density and temperature have a significant effect on the liquid phase penetration, while the injection pressure has no significant effect on the maximum liquid phase penetration.

Schematic diagrams and main components of the equipment, experimental layout for imaging tests, instantaneous spray images, example of the liquid phase penetration for different nozzle holes, injection pressures, different gas density and temperature are presented in the paper.

Keywords: *direct injection, liquid phase, thermal engine, break-up time*

1. Introduction

Improvement of the Diesel engine combustion processes to meet emission regulation is currently considered as a major objective. Following this path, it is important to understand the in-cylinder processes in direct-injection Diesel engines, where the impingement of liquid fuel on the piston bowl and other in-cylinder walls can lead to greater emission. Moreover, the liquid phase penetration characterizes the processes of atomization and vaporization, and so the air-fuel mixing processes. As a result, understanding how various parameters affect the penetration of the liquid-phase fuel in a diesel spray is important for combustion systems designers. The main goal of this paper is to propose a statically correlation for the maximum penetration distance of liquid phase fuel in a diesel spray, defined as the liquid phase (*LL*).

The development of the phenomenological study is based on recent experimental results obtained with an engine with an optically accessible cylinder head [1, 9].

2. Experimental equipment

The experimental equipment allows one to study the injection-combustion process under thermodynamic conditions (pressure, temperature and density) at top dead centre (TDC) similar as those existent in current direct injection Diesel engines. The main component is a single cylinder port-scavenging two-stroke engine with three-litre displacement and low rotational speed (~500 rpm). Geometrical characteristics are presented in Table 1. The engine cycle has no net power output, as injected fuel quantities are not high enough to maintain the engine running. Accordingly, the engine needs to be motored. However, the piston compression – expansion strokes are used to obtain realistic in-cylinder thermodynamic conditions in which injection-combustion processes can be studied.

Tab. 1. Two stroke engine geometrical characteristics

Bore	150 [mm]
Stroke	170 [mm]
Displacement	3 [L]
Effective Compression Ratio	17.1:1

Due to the necessity of studying the spray injection process under both inert and reacting conditions, the setup has the possibility to switch between two possible inlet atmospheres:
- Inert atmosphere, in which pure nitrogen is supplied to the engine as intake gas, due to its similarity with pure air. Figure 1 shows a schematic of the whole setup and the monitoring equipment under this configuration. The engine runs in a closed-loop circuit: intake nitrogen is blown by a Roots compressor through two conditioning units and a small settling chamber into the two-stroke engine. After injection, exhaust gases (i.e., fuel and nitrogen) are cooled down and filtered by a system that separates back fuel droplets and eliminates any solid particulate. The resulting clean nitrogen atmosphere is conducted back into the Roots compressor intake, filling the circuit with nitrogen compensates for possible leakages.
- Reacting atmosphere, in which room air is supplied to the Roots compressor, and after compression it is conducted to the intake of the two stroke engine as in the inert atmosphere configuration. Combustion gases are exhausted back to the atmosphere, as in a conventional engine. Figure 2 shows a schematic of the setup and monitoring equipment under this configuration.

The first configuration will be referred to as ‘closed loop’ configuration, and is used to analyze the spray injection, atomization and evaporation processes, whereas the second one will be called ‘open loop’ configuration, and is used to study the combustion process.

This result is very significant when we take into consideration that it has been achieved only due to a better regulation of the engine cylinders filling by means of a variable timed valve gear, without any change of the engine dimensions, compression ratio or maximum value of rotational speed.

Combustion Chamber Description

Figure 3 shows a schematic of the combustion chamber and the cylindrical injection chamber (45 mm diameter and 55 mm height). The injection chamber has four lateral windows, with one of them holding a pressure transducer. The injector is located on the upper wall. The 49 × 33 mm lateral windows consist of 20 mm thick quartz blocks. Details of the cylinder head can be observed in Figure 3.

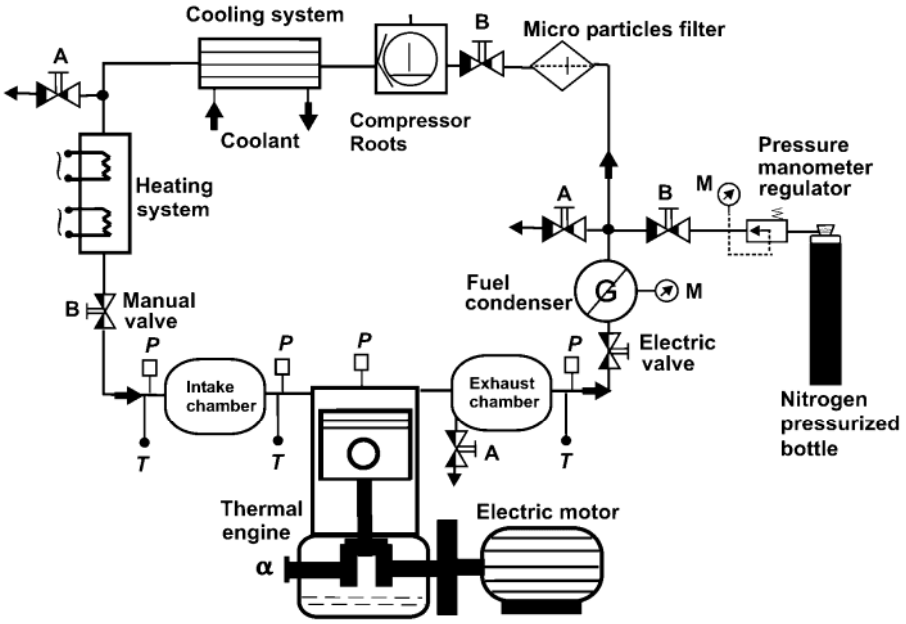

Fig. 1. Schematic diagram and main components of the equipment running under closed-loop configuration, (i.e. intake gas is nitrogen)

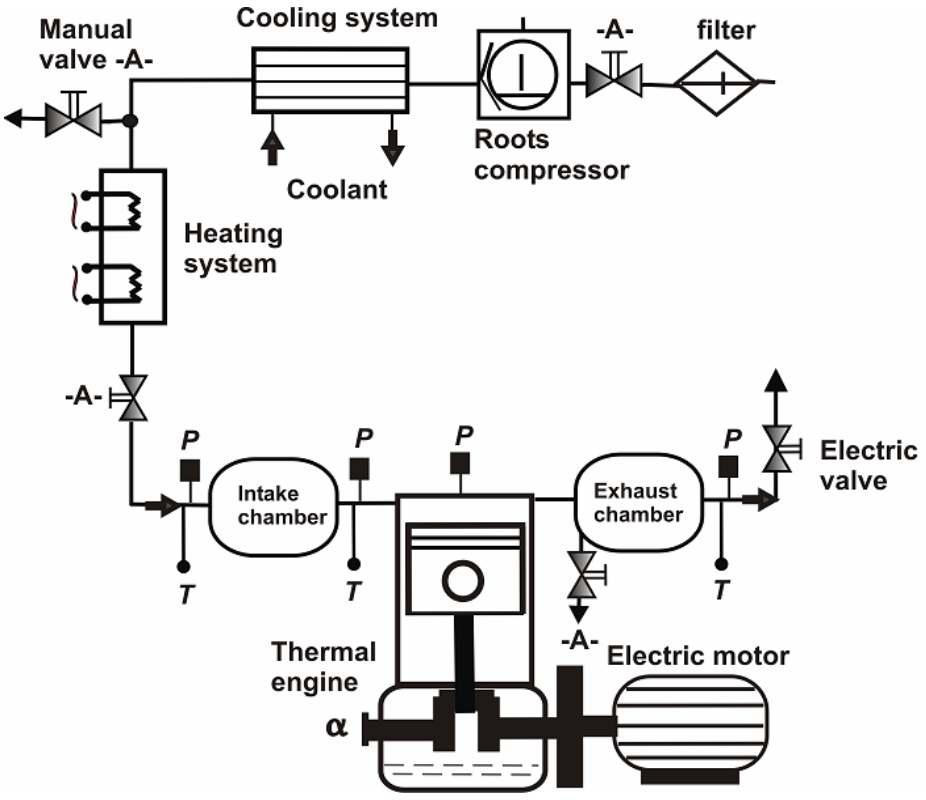

Fig. 2. Schematic diagram and main components of the equipment running under open-loop configuration, (i.e. intake gas is air)

Injection System

We use a Bosch common rail injection system that operates between 300 and 1300 bar. The injector uses a mini sac nozzle with a single axisymmetric hole, whose diameter varies from 115 to 200 μm. The injection system permits variation of important parameters like injection timing,

pressure and frequency. The injection events being analyzed last 1, 5 ms. Fuel is injected every 12 cycles to keep the windows clean for better imaging.

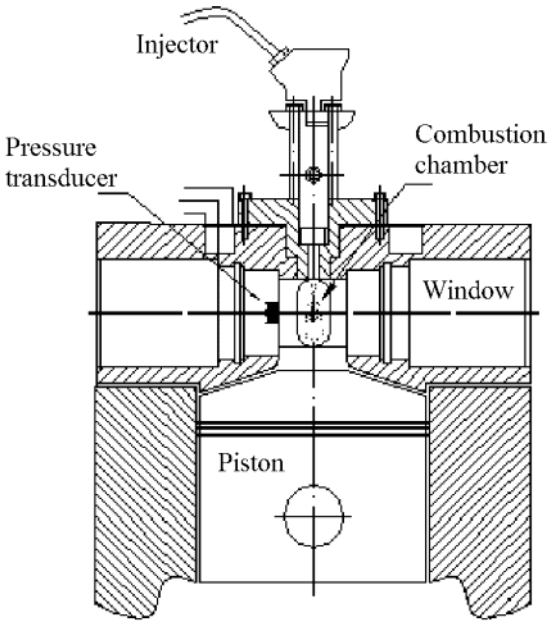

Fig. 3. Cross-sectional view of cylinder head

Engine Operating Conditions

The engine is operated at a constant 500 rpm speed, which is optimum for testing and measurement because it minimizes lubrication and vibration issues. The quartz optical surfaces are estimated to resist up to 120 bar, and peak cylinder pressure is kept between 60 and 80 bar. The engine block temperature is maintained at a fixed temperature during all the experiments with external heater and cooler devices. An intake heater can control intake temperatures at any value between 25 and 120 °C. Intake conditions are continuously monitored.

Experimental Conditions

The following table present the different experiments performed. Table 2 shows the variations of the nozzle hole diameter, injection pressure, intake gas temperature and intake gas pressure for inert atmosphere study.

Tab. 2. Variations of the injection parameters and thermodynamics conditions

Diameter of nozzle	115 - 130 - 170 – 200 [μm]
Injection pressure	300 - 700 - 1100 - 1300 [bar]
Intake gas temperature	333- 343 - 359 [K]
Intake gas pressure	~1,19 ~1,38 ~ 1,65 [bar]

The calculation of the density of gas at TDC in the combustion chamber is based on the gas pressure and temperature in the chamber at TDC and the specific constant gas of nitrogen (R = 296.78 J/kg-K).

The instantaneous pressure in the chamber at TDC was monitored with a piezoelectric instantaneous transducer (Kistler 6067B) placed in an access of the cylinder head (see figure 2). Another piezorresistive instantaneous transducer (Kistler 4045A5) placed between the small intake settling chamber and the cylinder (see Figure 1) allows the admission pressure at BDC to be known. A temperature sensor is situated at the same place and measures the temperature of admitted nitrogen at BDC.

Determination of the gas temperature and density in the chamber during the image acquisition period. The average gas temperature and density during the image acquisition period were determined from the conditions at the start of injection with the following relationship for polytrophic compression:

$$T_g = T_{soi}\left(\frac{P_a}{P_{soi}}\right)^{\frac{n-1}{n}}, \tag{1}$$

$$T_{soi} = T_{\alpha}\left(\frac{P_{soi}}{P_{\alpha}}\right)^{\frac{n-1}{n}}, \tag{2}$$

$$\rho_g = \rho_{soi}\left(\frac{P_a}{P_{soi}}\right)^{\frac{1}{n}}, \tag{3}$$

$$\rho_{soi} = \frac{P_{soi}}{R \cdot T_{soi}}, \tag{4}$$

where:

T_{soi} - Temperature at start of injection,
P_{soi} - Pressure at start of injection,
ρ_{soi} - Density at start of injection,
T_g - Temperature of the gas during the image acquisition period,
P_g - Pressure of the gas during the image acquisition period,
ρ_g - Density of the gas during the image acquisition period,
P_a - Measured chamber pressure during imaging acquisition period,
n - 1.33.

Image Acquisition Configuration

The experimental equipment consists basically of a Xenon stroboscopic light source, a light diffuser and a colour CCD camera.

Images acquired are the result of the attenuation through the spray of light emitted from an external source. This attenuation, at least in the case of diesel sprays, is produced mainly by liquid droplet scattering.

Images are collected by the CCD camera located in front of the window on the opposite side of the combustion chamber. The camera has a pixel resolution of 768 x 484 and a shutter speed of 1/16000.

This technique is suitable for studying the periphery contour of the liquid spray, thus yielding information on its macroscopic characteristics. Measurable parameters are those derived from the detection of the liquid phase outer contour (i.e. the liquid length). For contour detection, images are processed with purpose-developed image processing algorithms described in [11] on the bases of LRT segmentation methods to discriminate between spray and background.

Experimental Layout

The experimental equipment and layout is presented in Figure 4. It consists basically of a Xenon stroboscopic light source, a light diffuser and a colour CCD camera. Light pulses from the light source have a 20 μs duration at 1/3 peak of light pulse. They are directed by a combination of optical fibres and one lens onto a diffuser before travelling through one of the windows into the combustion chamber. Images are collected by the CCD camera located in front of the window at the opposite side of the combustion chamber. The camera (Pulnix TMC9700) has a pixel resolution of 768 x 484, and a dynamic range of 8 bits per colour channel. A Nikon conventional objective, which is suitable for the visible range, is used for the tests, with 60 mm focal length. The system image acquisition and synchronization with the injection event is controlled by commercial hard- and software (AVL Video-system 513D).

Images were acquired at 60 μs intervals from the start of injection. For every time position, 10 images were acquired from different cycles in order to obtain a representative sample of results. With the optics employed, the spatial resolution of the images was 16 pixels/mm. The images effective exposure time is controlled by the light pulse duration (20 μs), which is much shorter than the minimum camera exposure time.

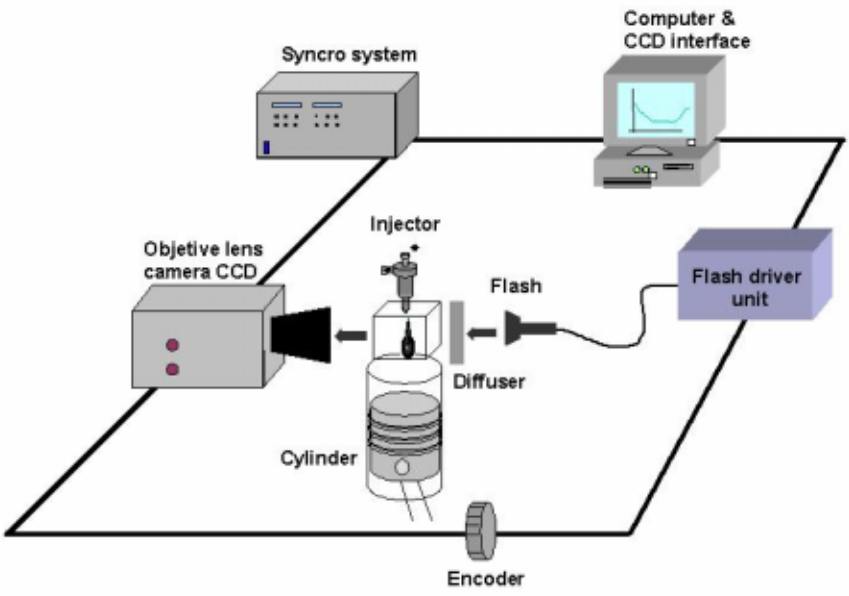

Fig. 4. Experimental layout for ombroscopy imaging tests

3. Results

Figure 5 shows a sample of instantaneous images acquired by means of this imaging technique. As commented, light is attenuated through the spray by liquid droplets. As a result, the dark area in the images corresponds to the location of the spray liquid phase. Figures at the bottom of the

images correspond to time elapsed from the start of injection, defined as the last time for which no spray can be imaged with a resolution of 60 μs.

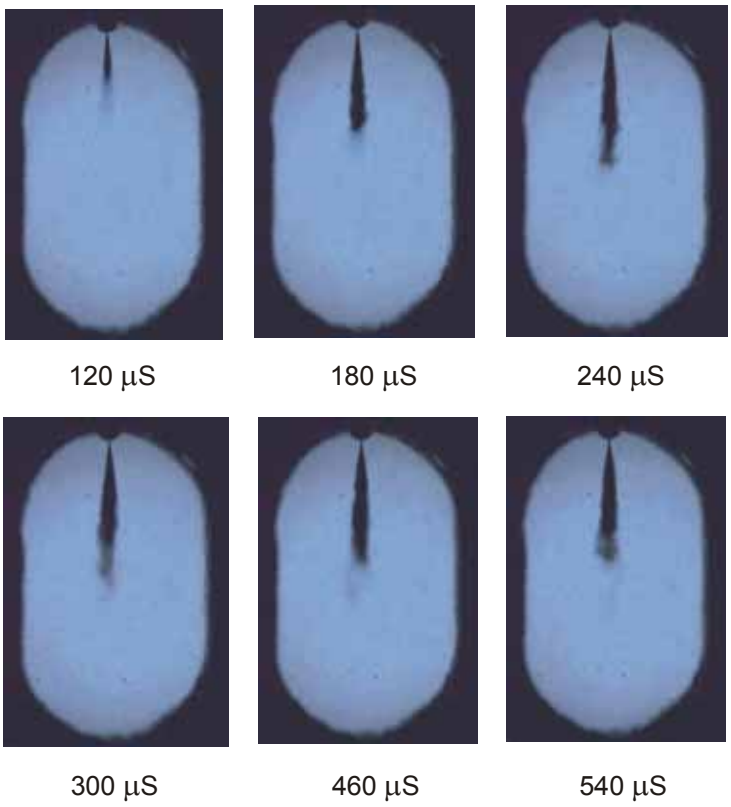

Fig. 5. Instantaneous ombroscopy images

The images show how the liquid spray penetrates across the combustion chamber, reaching a maximum extent after about 240 μs, the so-called "maximum liquid length or liquid phase". No more liquid can be observed downstream of this position. This results from the fact that spray entrains the necessary energy from the environment in order to vaporize all fuel after a certain distance from the nozzle exit, as has often been found in literature [3-13]. Despite the fact that vapour phase cannot be studied with this simple technique, images in which the maximum liquid length has been attained show that the liquid phase starts developing in a cone-like shape just beside the nozzle. After a very short distance from the nozzle compared to the total liquid length, the liquid phase contour limits do not grow anymore in the direction perpendicular to the spray axis, losing their cone-like shape. Figure 5 shows - instantaneous ombroscopy images.

Liquid spray width becomes almost constant for longer distances from the nozzle until close to the tip, where it shrinks. As spray width usually grows linearly in proportion to the axial distance, this observation should indicate that vapour phase has already appeared, and that it is progressing far away from the liquid phase, maintaining a linear growth of the spray total (liquid and vapour) width as distance from the nozzle increases.

The Figure 6, for example, shows the results from the image processing algorithms in terms of the liquid spray penetration evolution. The plot symbols represent the average result from the processing of the 10 instantaneous images for every time position. An error example (figure 6) bar has also been plotted for every time position that represents ± one standard deviation, in order to account for both turbulence fluctuations and cyclic dispersion from the injection system.

For every test case, penetration curves show how liquid phase increases steadily during the first part of the injection process until reaching a maximum value after a time position that depends on the particular test conditions.

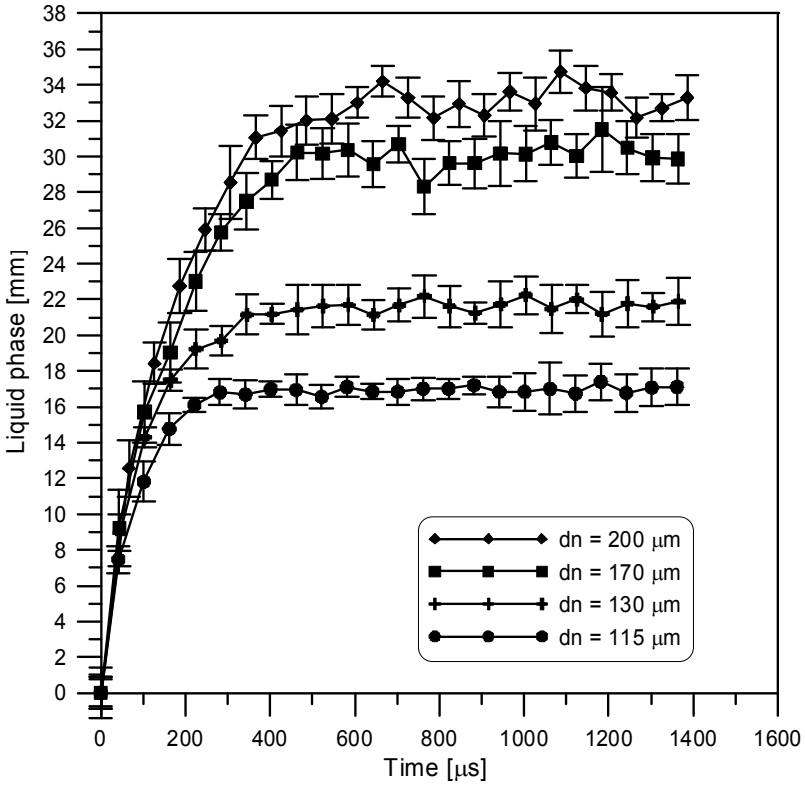

Fig. 6. Example of the liquid phase penetration for different nozzle hole diameters. Injection pressure (1300 bar), density (26 kg/m3) and gas temperature (906 K) are constant during the test

Phenomenological characterization of the liquid phase penetration

-Nozzle hole diameter influence

The experimental test of the table 3 are plotted in the figure 7, this shows a dominant trend: reducing the nozzle hole diameter decreased the maximum liquid phase, principally for a major involving gas entrainment relative to mass fuel flow for the same axial distance [5, 14], and a better atomization caused for the size droplets reduction in the diesel spray [6]. The maximum liquid phase considered in figure 7 is the mean value of liquid phase after the initial transient growing period. The mean penetration dependence on the nozzle hole diameter calculated is $LL \equiv Kdn^{1,13}$ ($R^2 = 94\%$). This exponent is higher but close to the one reported by Naber [10], who observed that the liquid phase decreases linearly with the nozzle hole diameter reductions.

Tab. 3. Experimental test for the determination of the nozzle hole diameter and injection pressure influence

Injection pressure [bar]	Nozzle hole diameter [μm]	Gas density [kg/m^3]	Gas temperature [K]
300	115	26	906
700	130	26	906
1100	170	26	906
1300	200	26	906

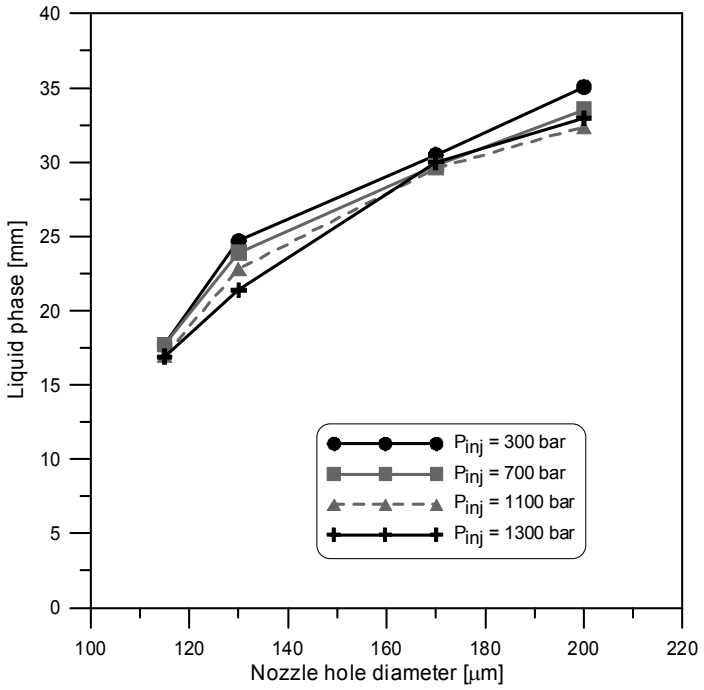

Fig. 7. Maximum liquid phase penetration for different injection pressure according to the nozzle hole diameter

- Injection pressure influence

An example of the influence of the injection pressure is shown by the figure 8. These figure shows that injection pressure has no significant effect on the maximum liquid phase penetration. It is also depicted that higher injection pressure gives faster liquid spray penetration until the maximum liquid phase value is achieved, due to the higher increased penetration velocity which is finally compensated by the faster mixing injection process.

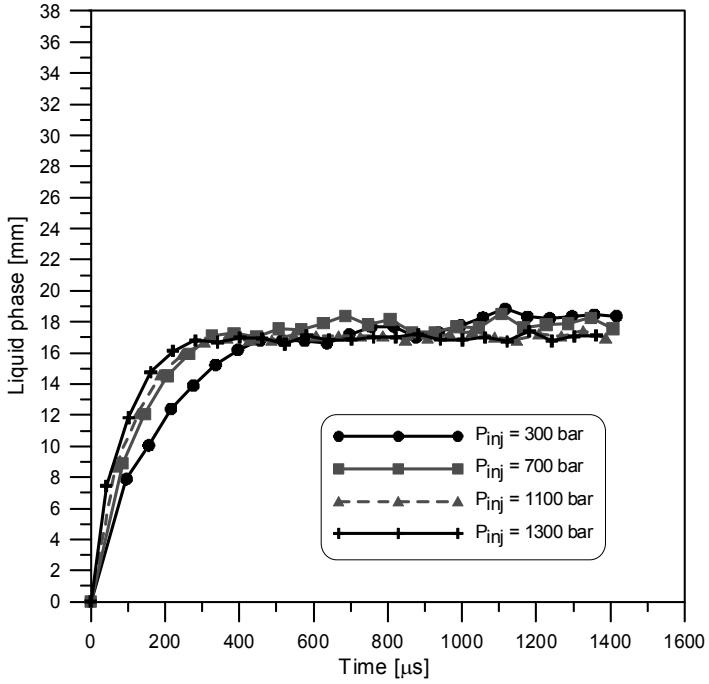

Fig. 8. Example of the Liquid phase penetration for different injection pressures and the same nozzle hole diameter (115 μm). The gas density (26 kg/m3) and the temperature in the chamber (906 K) are constant during the test

The experimental test is shown in the table 3 and the global results are plotted in the figure 9. This figure shows the trend for the mean value. The penetration depends on $LL \equiv KP_{inj}^{-0,06}$ (R^2 = *96%*), which is negligible, as well as reported by Siebers [14]. Increasing the injection pressure causes an increase of the mass flow rate and of the injection velocity. These effects tend towards lengthening the liquid phase. But they also cause a faster atomization and a faster mixing, because of the increase on air entrainment and the reduced average size of the drops. These opposite effects cancel each other out, and so the maximum liquid phase is almost unchanged.

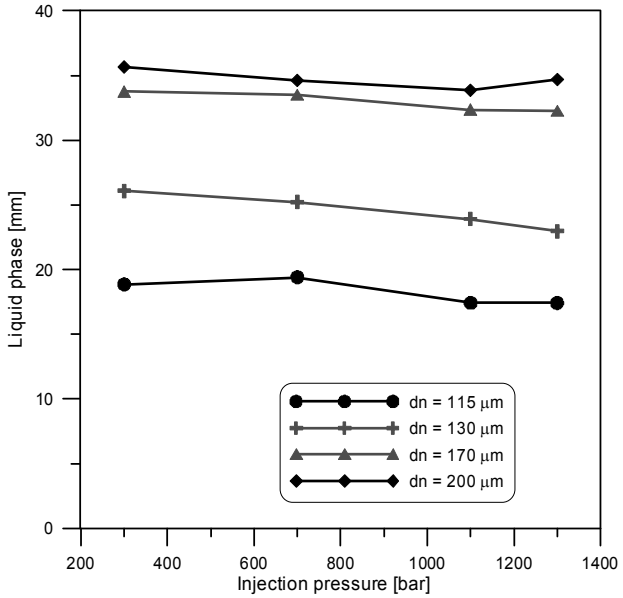

Fig. 9. Maximum liquid phase penetration for different nozzle hole diameters according to the injection pressures

- Gas density at the top dead centre influence

The experimental test is shown in the table 4. The general trend is a decrease in the liquid phase penetration with an increase in ambient density, as shows in the figure 10. The Figure 11 shows the tendency for the mean value. The mean penetration dependence on density calculated is $LL \equiv K\rho_g^{-0,52}$ (R^2 = *98%*). This behaviour is caused by ambient gas density effects on spray dispersion (i.e. air entrainment) as noted by Naber [10]. The larger entrained mass leads to a slower penetration velocity and reduced penetration.

Tab. 4. Experimental test for the determination of the gas density influence

Injection pressure [bar]	Nozzle hole diameter [μm]	Gas density $_{TDC}$ [kg/m^3]	Gas temperature $_{TDC}$ [K]
700	150	23	890
700	150	26,5	890
700	150	31,5	890
700	150	22	910
700	150	25.5	910
700	150	30	910
700	150	21	945
700	150	24,5	945
700	150	29	945

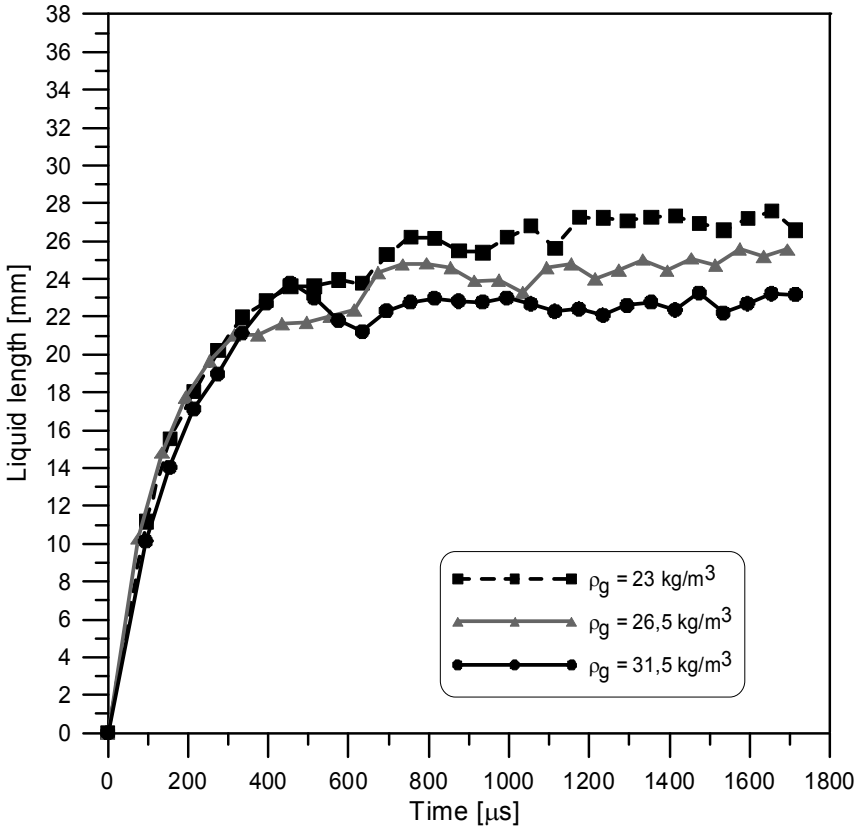

Fig. 10. Example of the liquid phase penetration for different gas density. The injection pressure (P_{inj} = 700 bar), nozzle hole diameter (150 μm) and gas temperature in the chamber (906 K) are constant during the test

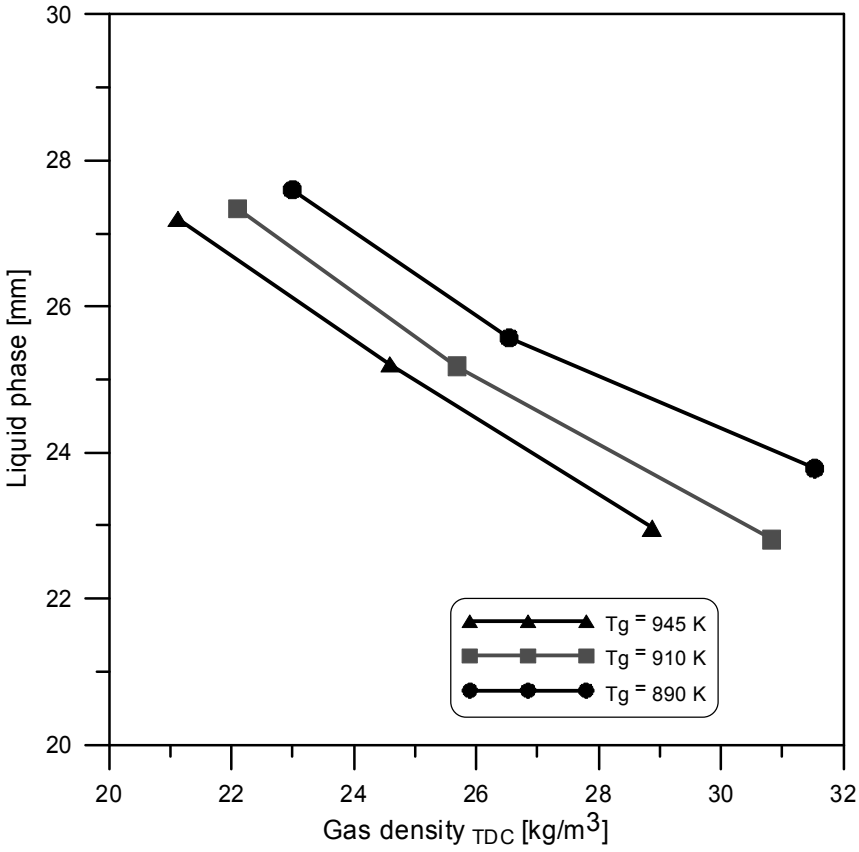

Fig. 11. Maximum liquid phase penetration for different gas temperatures according to gas density

- Gas temperature influence

The experimental characterization for the determination of the gas temperature influence on the liquid phase penetration is shows in the table 5. The general trend is a decrease in the liquid phase penetration with an increase in gas temperature, as shown in the figure 12.

The figure 13 shows the tendency for the mean value. The mean penetration dependence on gas temperature calculated is $LL \equiv KT_g^{-1,4}$ (R^2 = 99%). This behaviour is caused by the increasing evaporating fuel rate, the test show that the increase of the gas temperature reduce the maximum liquid phase penetration, principally at high pressure, the cause is that the fuel rate and the speed penetration is greatest at high pressure while at low pressure is the opposite. The high gas temperature in the combustion chamber at star of injection in a real combustion engine is benefit because these cause a delay in the start of combustion and burn fraction [3].

Tab. 5. Experimental test for the determination of the gas temperature influence

Injection pressure [bar]	Nozzle hole diameter [μm]	Gas density $_{TDC}$ [kg/m^3]	Gas temperature $_{TDC}$ [K]
1100	150	20,54	857,78
1100	150	19,36	896,47
1100	150	18,37	936,19
700	150	20,34	855,05
700	150	19,28	895,24
700	150	18,29	934,94
300	150	20,13	852,16
300	150	18,93	889,79
300	150	17,99	929,85

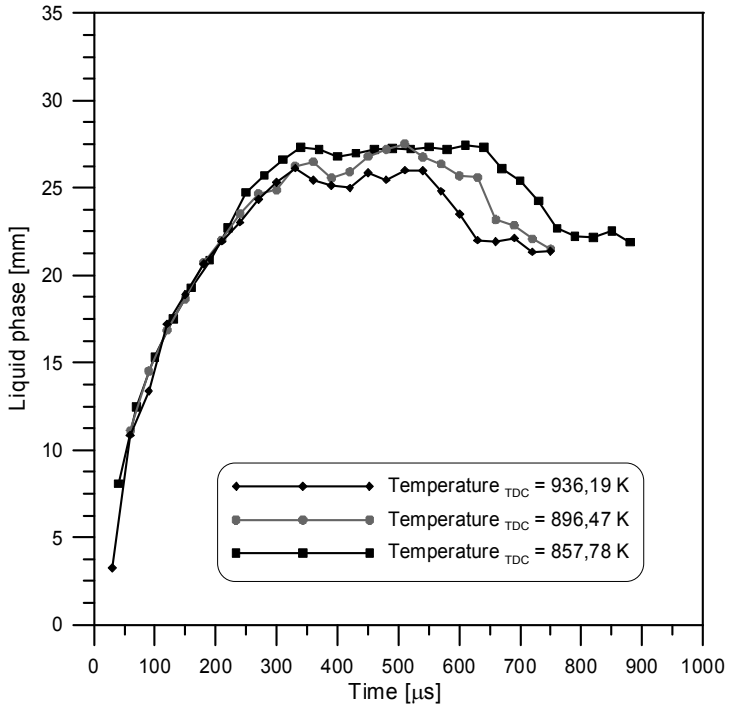

Fig. 12. Example of the liquid phase penetration for different gas temperature. The injection pressure (P_{inj} = 1100 bar) and nozzle hole diameter (150 μm) are constant during the test

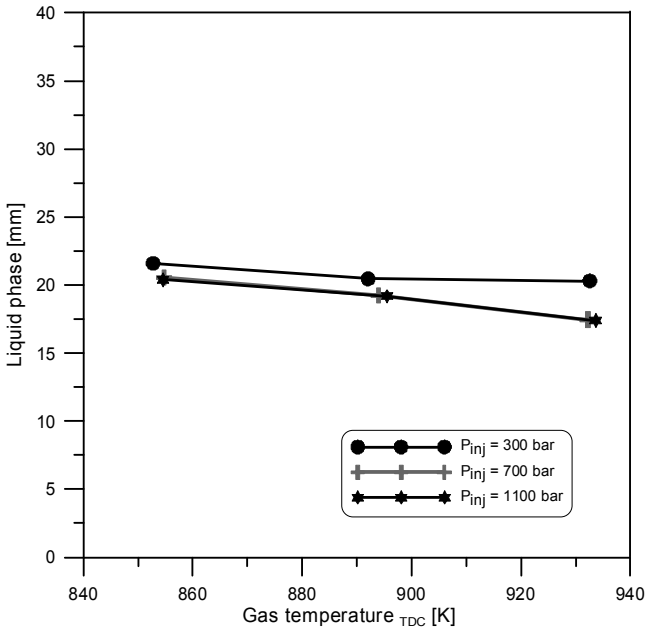

Fig. 13. Maximum liquid phase penetration for different injection pressures according to gas temperature

4. Summary and conclusions

Experimental measurements were carried out to estimate the liquid phase penetration of a diesel fuel jet injected in an inert and reactive environment. The effects of the characteristic parameters, i.e. the nozzle hole diameter, injection pressure, density and gas temperature were analyzed. The transient fuel injection process was recorded using optical access, and the liquid phase penetration was measured using the ombroscopy technique.

The trends observed in the effects of these parameters on the liquid phase in an evaporating diesel spray are:

- Nozzle hole diameter is the most influential parameter. Decreasing this diameter causes a slower penetration and a quicker second atomization break-up, which leads to a shorter maximum liquid phase penetration.
- Increasing injection pressure also prompts a faster penetration and a quicker atomization break-up, but has no significant effect on maximum liquid phase. The lengthening effect of velocity and the shortening effect of atomization and vaporization cancel each other out, which explains this lack of dependence.
- Ambient gas density and temperature have strong effects on liquid phase. An increase in gas density or temperature causes a decrease in the liquid phase penetration. The sensitivity of liquid phase to both parameters nevertheless decreases as they increase, markedly so far gas density. The rising in density of gas in the chamber slows down liquid phase penetration and delays the second atomization break-up. It results in a reduced penetration and a shorter liquid phase.

Liquid phase penetration behaviour can be controlled through the parameters investigated. Nozzle hole diameter seems to be the more accessible and the most influential one. Reducing the orifice size leads to a faster atomization and a reduced maximum liquid phase, which are both predisposing factors to avoid wall impingement problems and to improve air–fuel mixing processes. But practical limits exist on the minimum orifice size that can be made and on the degree to which fuel can be filtered to prevent orifice plugging. Moreover, the drop in the injection rate caused by the reduction in the exit orifice can be made up by increasing injection pressure (i.e.

pressure drop) which has a very limited decrease effect on liquid phase, keeping in mind that technical limits also exist.

References

[1] Araneo, L., *Prediction of Diesel Spray Penetration with Short Injections in Low Density Gas* Proceedings of Conference on Thermo- and Fluid-Dynamic Processes in Diesel Engines, THIESEL, Spain 2004.

[2] Bermúdez, V. García, J. M., Juliá, E. Martínez, S., *Engine with Optically Accessible Cylinder Head: a Research Tool for Injection and Combustion Processes*, SAE Paper 2003-01-1110, Detroit 2003.

[3] Christoph, E. and Dec, J. E., *The effect of TDC Temperature and Density on the Liquid-Phase Fuel Penetration in a D. I. Diesel Engine,* SAE Paper 952456, Toronto 1995.

[4] Dent, J. C., *A Basis for the Comparison of Various Experimental Methods for Studying Spray Penetration*, SAE Transaction, Vol. 80 (1971), SAE Paper 710571, Detroit 1971.

[5] Desantes, J. M., Pastor, J. M., Martínez, S. and Riesco, J. M., *Experimental Characterization of the Liquid Phase Penetration on Evaporating Diesel Sprays*, SAE Paper 2005-01-2095, Brasil 2005.

[6] Hiroyasu, A. and Arai, M., *Structures of Fuel Sprays in Diesel Engine*, SAE Paper 900475, Detroit 1990.

[7] Hodges, J. T., Baritaud, T. A. and Heinze, T. A. *Planar liquid and gas fuel and droplet size visualization in a DI Diesel engine*, SAE Paper 910726, Detroit 1991.

[8] Kamimoto, T., Yokota, H., and Kobayashi, H., *Effect or High Pressure Injection on Soot Formation Processes in a Rapid Compression Machine to Simulate Diesel Flames*, Transactions of the SAE, Vol. 96, Sect. 4, pp. 4783-4791, Detroit 1987.

[9] Martínez, S., *Development of an Experimental Set-up for Study of the Evaporated Diesel Sprays on Inert and Reactive Atmosphere,* PhD Theses, UPV, Spain 2003.

[10] Naber, J. D. and Siebers, D. L., *Effect of Gas Density and vaporization on Penetration and Dispersion of Diesel Spray*, SAE Paper 960034, Detroit 1999.

[11] Pastor, J. V., Arrègle, J., Palomares, A., *Diesel Spray Image Segmentation with a Likelihood Ratio Test*, Applied Optics 40, 1-10, UK 2001.

[12] Pauer, T., Wirth, R. and Brüggemann, D., *Time resolved Analysis of Mixture Preparation and Ignition by Combined Optical Measurement Techniques for DI-Diesel Injection Nozzle in a High Pressure- / High Temperature Chamber*, AVL 4th. International Symposium on Internal Combustion Diagnostics, Baden-Baden 2000.

[13] Payri, F., Desantes, J. M. and Arrégle, J., *Characterization of D.I. Diesel Sprays in High Density Conditions*, SAE Paper 960774, Detroit 1996.

[14] Siebers, D.L., *Liquid-Phase Fuel Penetration in Diesel Sprays*", SAE Transactions, Vol. 107, Sec. 3, pp. 1205-1227, SAE Paper 980809, Detroit 1998.